

Posterior Regularisation on Bayesian Hierarchical Mixture Clustering

Wěipéng Huáng · Tin Lok James Ng ·
Nishma Laitonjam · Neil J. Hurley

Received: date / Accepted: date

Abstract We study a recent inferential framework, named posterior regularisation, on the Bayesian hierarchical mixture clustering (BHMC) model. This framework facilitates a simple way to impose extra constraints on a Bayesian model to overcome some weakness of the original model. It narrows the search space of the parameters of the Bayesian model through a formalism that imposes certain constraints on the features of the found solutions. In this paper, in order to enhance the separation of clusters, we apply posterior regularisation to impose max-margin constraints on the nodes at every level of the hierarchy. This paper shows how the framework integrates with BHMC and achieves the expected improvements over the original Bayesian model.

1 Introduction

Posterior regularisation (PR) is an emerging approach to handle Bayesian models with extra constraints. The framework is founded on an approach of minimising the Kullback-Leibler (KL) divergence between a variational solution and the posterior, in a constrained space. The works (Dudík et al., 2004, 2007; Altun and Smola, 2006) first raised the idea of including constraints in maximum entropy density estimation and provided a theoretical analysis. Based on *convex duality* theory, the optimal solution of the regularised posterior is found to be the original posterior of the model, discounted by the constrained pseudo likelihood introduced by the constraints.

Later work founded on the idea of posterior constraints includes (Graça et al., 2009) which proposed constraining the E-step of an Expectation-maximization (EM) algorithm, in order to impose feature constraints on the solution. Around the same

W. Huang · N. Laitonjam · N. J. Hurley
Insight Centre for Data Analytics, University College Dublin, Dublin, Ireland
E-mail: {firstname.lastname}@insight-centre.org

T.L.J. Ng
School of Computer Science and Statistics, Trinity College Dublin, Dublin, Ireland
E-mail: ngja@tcd.ie

time, [Zhu and Xing \(2009\)](#) proposed structural maximum entropy discrimination Support Vector Machines (SVM), which use the same idea. A number of extensions to various models have been proposed, including to SVM, Matrix Factorisation, Topic Models, Classification, Regression and Clustering etc. ([Zhu et al., 2011, 2012](#); [Xu et al., 2012](#); [Zhu et al., 2014a](#); [He et al., 2020](#); [Chen et al., 2014](#)), which can all be developed under the common framework of Posterior Regularisation ([Dudík et al., 2004, 2007](#); [Altun and Smola, 2006](#); [Ganchev and Gillenwater, 2010](#); [Zhu et al., 2014b](#)). However, we notice that most works are within the category of supervised learning.

As mentioned in ([Graça et al., 2009](#)), extending generative models to incorporate even small additional constraints is practically challenging. In comparison, posterior regularisation is a considerably simpler and more flexible means of learning models with extra information. In short, it maintains the properties of the original model while constraining the solution search to a restricted space. For example, the *max-margin* Bayesian clustering (MMBC) model ([Chen et al., 2014](#)) imposes a latent linear discriminant variable on a Dirichlet Process Mixture Model (DPMM) to ensure that clusters are better separated. The framework adds discounts to the likelihood for each individual datum, i.e. it adjusts the proportion of each cluster assignment for every datum. On the other hand, it does not alter any other bit of the DPMM itself. In contrast, the Bayesian Repulsive Gaussian Mixture Model (BRGM) was proposed by ([Xie and Xu, 2020](#)) and performs a similar job to MMBC but imposes the constraints on the prior rather than the likelihood. In particular, the BRGM imposes a distance function between the Gaussian clusters in the generative process. Designing such a novel model (BRGM) needs careful consideration about the posterior consistency. Also, it loses exchangeability which leads to harder inference procedures. So far, only a Gaussian model and simple distance function are applied and analysed—there is still much to explore for this stream of models with other distributions and distance functions.

1.1 Bayesian Hierarchical Clustering

Our focus is to enhance the Bayesian hierarchical mixture clustering (BHMC) ([Huang et al., 2021](#)) model. Here, each node in the hierarchy is associated with a distribution, with parameters connected through a transition kernel along paths in the hierarchy. Each datum is generated by choosing a path through the hierarchy to a leaf node and is then drawn from the distribution associated with the leaf.

One significant property of the BHMC model is that the nodes in the hierarchy/tree¹ are associated with a mixture model rather than a Gaussian distribution, which is the more common choice in Bayesian hierarchical clustering ([Adams et al., 2010](#); [Neal, 2003](#); [Knowles and Ghahramani, 2015](#)). That is, the parent-to-node diffusion in the BHMC is a multi-level Hierarchical Dirichlet Process Mixture Model (HDPMM). With proper hyperparameter settings, the non-zero mixture components will reduce for nodes that are deeper in the tree.

We aim to apply posterior regularisation to the BHMC model. Consider that at any level of the hierarchy, each node in the BHMC corresponds to some mixture distribution. Inspired by a recent evaluation framework on hierarchies ([Huang et al.,](#)

¹ In this paper, we will use the term “hierarchy” and “tree” interchangeably

2020), we recognise that a good hierarchy should exhibit good separation, particularly at high levels, close to the root. This means that the mixture components associated with each node should be geometrically close together, relative to their separation from the components associated with the other nodes on the same level. However, we find that an inference procedure over the model can easily get stuck in a local mode where the components associated with high level nodes are not sufficiently coherent. We attribute this to the fact that the data is generated only at the leaf nodes, so that it can take a long time for the data to influence the mixture components at the higher levels. Separation of the mixture components among nodes at the same level is a desirable feature of the posterior and our solution is to regularise the model in order to focus the optimisation on distributions that exhibit this feature. In practise, regularisation has the impact of introducing an explicit data dependence on the choice of mixture components at every level, pushing the direct influence of the data up to all levels along every path in the hierarchy. Specifically, we add the *max-margin* property to the nodes at each level, such that the decision boundary determining the correct node for each datum is maximally separated from the other nodes. As suggested in (Ganchev and Gillenwater, 2010), the constraints should contain features that appear nowhere in the original model; therefore, *max-margin* in the internal nodes and BHMC can be a good marriage under the framework of PR.

1.2 Why max-margin for HC?

HC is inherently an unsupervised learning problem that learns the latent labels for the data. In particular, it assigns a sequence of dependent labels to each datum. Huang et al. (2020) suggest that a high quality hierarchy should be separated sufficiently well under each parent so that a robot can easily identify where each datum belongs and then retrieve the datum. It is non-trivial to formulate such separating features, but we can appeal to an approximation by introducing *max-margin* to the original model. Starting from the simplest SVM binary classification, we consider a datum $\mathbf{x}_n \in \mathbf{X} = \{\mathbf{x}_1, \dots, \mathbf{x}_N\}$ could be assigned with a label v_n where $v_n \in \{-1, 1\}$. Now, we augment it with a latent discriminant variable $\boldsymbol{\eta}$ so that

$$v_n \left(\boldsymbol{\eta}^\top \mathbf{x}_n + \eta_0 \right) > \epsilon/2 \implies \begin{cases} (\boldsymbol{\eta}^\top \mathbf{x}_n + \eta_0) > \epsilon/2 & v_n = 1 \\ -(\boldsymbol{\eta}^\top \mathbf{x}_n + \eta_0) > \epsilon/2 & v_n = -1 \end{cases}.$$

Thus, $\boldsymbol{\eta}^\top \mathbf{x} + \eta_0$ (for a certain \mathbf{x}) is the hyperplane boundary that separates the two classes, and the datum on the two sides are at least $\epsilon/2$ units away from the hyperplane (Hastie et al., 2009). Simplifying the case, we set η_0 as constant. Using a non-negative slack variable ξ_n for n , we write

$$v_n \left(\boldsymbol{\eta}^\top \mathbf{x}_n + \eta_0 \right) > \epsilon/2 - \xi_n/2.$$

However, when there are more than two classes, which is common for clustering, we need some modifications. One way is to associate a different $\boldsymbol{\eta}$ with each cluster. This $\boldsymbol{\eta}$ can be then employed to form a boundary to separate the data in this cluster and the rest (namely, the one-vs-all approach (Hsu and Lin, 2002)). We set

the cluster assignment v_n to be 1 and set any other cluster to be -1 . Considering a class denoted with z or z' , the optimisation will have the following constraints:

$$\begin{cases} (\boldsymbol{\eta}_z^\top \mathbf{x}_n + \eta_0) > \epsilon/2 - \xi_n/2 & z = v_n \\ -(\boldsymbol{\eta}_{z'}^\top \mathbf{x}_n + \eta_0) > \epsilon/2 - \xi_n/2 & \forall z', z' \neq v_n \end{cases} \\ \implies \text{constraint space for datum } n = \left\{ (\boldsymbol{\eta}_{v_n} - \boldsymbol{\eta}_z)^\top \mathbf{x}_n > \epsilon - \xi_n \mid \forall z \neq v_n \right\}. \quad (1)$$

Our work extends this idea to a multilevel case to fit the task of HC, where the constraint can be applied to clusters under the same parent. Given the constraint space, we can then apply PR to restrict the search space for the Bayesian inference.

1.3 Contributions

In this paper, we analyse the modelling of PR with Bayesian HC which is studied for the first time. We show the improvements in the model given the extra components added to the model via *max-margin* and PR.

2 Preliminaries

We denote the tree by $\mathcal{H} = (Z_{\mathcal{H}}, E_{\mathcal{H}})$ where $Z_{\mathcal{H}}$ is the set of nodes and $E_{\mathcal{H}}$ is the edge set in the tree. For any $z, z' \in Z_{\mathcal{H}}$, we write $(z, z') \in E_{\mathcal{H}}$ if z is the parent of z' in the hierarchy. The paths can be collected through the set $\mathbb{Z}_{\mathcal{H}}$ which contains all paths. A path is an ordered list of nodes and therefore denoted by $\mathbf{z} = \{z_0, z_1, \dots, z_L\}$ such that $\mathbf{z} \in \mathbb{Z}_{\mathcal{H}}$ for all \mathbf{z} . Finally, we define $\mathcal{S}(z)$ to be the set of siblings of z such that $\mathcal{S}(z) = \{z' \mid z' \neq z, (z^*, z') \in E_{\mathcal{H}} \text{ where } z^* \text{ is the parent of } z\}$.

Dirichlet Process The BHMC relies heavily on the Dirichlet Process (DP). It has two well-known forms, namely the Chinese Restaurant Process (CRP) and the stick-breaking process. Given the n -th customer (datum) coming into a restaurant, in the CRP formulation, she would select a table k which is labelled as c_n . The randomness of CRP(α) is defined as

$$p(c_n = k \mid c_{1:n-1}, \alpha) = \begin{cases} \frac{N_k}{n+\alpha} & k \text{ exists} \\ \frac{\alpha}{n+\alpha} & k \text{ is new} \end{cases}$$

which means that the customer selects a table proportional to the number of customers (N_k) sitting at the table k while there is still a possibility to start a new table. The stick-breaking process simulates the process of taking portions out from a remaining stick. Assume the original stick is of length 1. Let o_k be the proportion of the length to be cut off from the remaining stick, and β_k be the actual length being removed. We can write

$$\beta_1 = o_1 \quad \beta_k = o_k \prod_{i=1}^{k-1} (1 - o_i) \quad o_i \sim \text{Beta}(1, \alpha)$$

and equivalently one can observe $p(c_n = k \mid \alpha) = \beta_k$. This is also known as the GEM distribution.

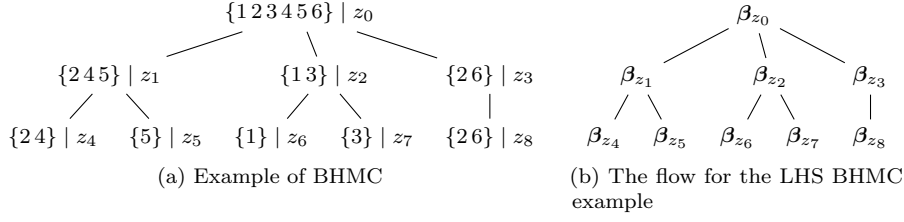


Fig. 1: An example of BHMC generative process

Nested Chinese Restaurant Process The CRP can be extended to a hierarchical random process, named the nested Chinese Restaurant Process (nCRP). Given a fixed hierarchy depth, L , the process recursively applies the CRP at each level. For a given data n , we denote the path assignment label of the datum in the hierarchy by \mathbf{v}_n , such that \mathbf{v}_n would be assigned with some $\mathbf{z} \in \mathbb{Z}_{\mathcal{H}}$.

Hierarchical Dirichlet Process Mixture Model (HDPMM) We summarise the content of (Huang et al., 2021) giving just the necessary details of the model. BHMC considers a hierarchy in which each node maintains a global book of mixture components, while keeping local weights for the components which can be completely different from each other.

Let H be a distribution, which we call the base measure. If G is drawn from a DP of G_0 such that $G \sim \text{DP}(\gamma, G_0)$ and $G_0 \sim \text{DP}(\gamma_0, H)$, then G is said to be an instance generated from a *hierarchical* DP (HDP) (Sudderth, 2006). In an HDPMM with finite K , the process to generate the n -th observation x_n is as follows:

$$\begin{aligned}
 \beta_1 \dots \beta_K \mid \gamma_0 &\sim \text{Dir}(\gamma_0/K \dots \gamma_0/K) & \theta_1 \dots \theta_K \mid H &\sim H \\
 \tilde{\beta}_1 \dots \tilde{\beta}_K \mid \gamma, \beta &\sim \text{Dir}(\gamma\beta) & c_n \mid \tilde{\beta} &\sim \text{Discrete}(\tilde{\beta}) \\
 x_n \mid c_n, \theta_1 \dots \theta_K &\sim F(\theta_{c_n})
 \end{aligned}$$

where $F(\cdot)$ is a sampling function that takes θ as its parameter.

Bayesian Hierarchical Mixture Clustering The model depicts the following generative process. Given an index n , the corresponding datum is generated through an nCRP with L steps, starting from the root node. Whenever a new node z is created during this nCRP, local weights of the global components are sampled from the node's parent through a HDP and associated with the node. After moving L times down the hierarchy, a leaf node is reached and the n -th observation is sampled using the local weights of the leaf node.

We show a generative example with a finite setting in Fig. 1 which has $K = 6$ and $L = 2$. The associated distributions are as follows:

$$\begin{aligned}
 \mathbf{v}_n &= \{z_0, v_{n1}, v_{n2}\} \sim \text{nCRP}(\alpha) \\
 \beta_0 &\sim \text{Dir}\left(\frac{\gamma_0}{K}, \dots, \frac{\gamma_0}{K}\right) \quad \beta_{v_{n1}} \sim \text{Dir}(\gamma\beta_0) \quad \beta_{v_{n2}} \sim \text{Dir}(\gamma\beta_{v_{n1}}) \\
 x_n &\sim F(\theta_{c_n}) \quad c_n \sim \text{Discrete}(\beta_{v_{n2}}) \quad \theta_1, \dots, \theta_K \sim H.
 \end{aligned}$$

For an infinite setting, we would instead sample $\mathbf{o} \sim \text{GEM}(\gamma_0)$ and thus acquire β_0 for the infinite setting. That is, $\beta_{z_0 k} = o_k \prod_{k'=1}^{k-1} (1 - o_{k'})$. For any node, we can present $\beta_z = \{\beta_{z1}, \dots, \beta_{zK}, \beta_z^*\}$ where the last element β_z^* is the probability of creating a new component. Then, for any $(z, z') \in E_{\mathcal{H}}$, we obtain $\beta_{z'} \sim \text{Dir}(\beta_z)$.

Algorithm 1 demonstrates a detailed generative process for the local variables, $\mathbf{v}_n = \mathbf{z}$ for some $\mathbf{z} \in \mathbb{Z}_{\mathcal{H}}$. Also, we can write $\mathbf{B}^- = \mathbf{B} \setminus \{\beta_{z_0}\}$ and thus obtain $p(\mathbf{B} \mid \gamma, \gamma_0) \equiv p(\mathbf{o} \mid \gamma_0) p(\mathbf{B}^- \mid \gamma)$. Let us denote the variables in the model by \mathbf{M}_0 such that $\mathbf{M}_0 = \{\mathbf{o}, \mathbf{B}^-, \mathbf{V}, \mathbf{c}, \Theta\}$. The variables are $\mathbf{B} = \{\beta_z\}_{z \in \mathcal{Z}_{\mathcal{H}}}$, $\mathbf{o} = \{o_k\}_{k=1}^{\infty}$, $\mathbf{V} = \{\mathbf{v}_n\}_{n=1}^N$, $\mathbf{c} = \{c_k\}_{k=1}^{\infty}$, and $\Theta = \{\theta_k\}_{k=1}^{\infty}$. Let $f(\cdot)$, corresponding to $F(\cdot)$, be the density function of x given the parameter θ . Moreover, $\mathbb{B}(\mathbf{a})$ is the beta function such that $\mathbb{B}(\mathbf{a}) = \prod_i \Gamma(a_i) / \Gamma(\sum_i a_i)$. With this notation, the model is summarised by Fig. 2.

```

1 Sample  $\beta_{z_0} \sim \text{GEM}(\gamma_0)$  //  $z_0$  is the root restaurant
2 Sample  $\theta_1, \theta_2, \theta_3, \dots \sim H$ 
3 for  $n = 1 \dots N$  do
4    $v_{n0} \leftarrow z_0$ 
5   for  $\ell = 1 \dots L$  do
6     Sample  $v_{n\ell}$  using  $\text{CRP}(\alpha)$ 
7      $z \leftarrow v_{n(\ell-1)}$ 
8      $z' \leftarrow v_{n\ell}$ 
9     if  $z'$  is new then
10      Sample  $\beta_{z'} \sim \text{DP}(\gamma, \beta_z)$ 
11      Attach  $(z, z')$  to the tree  $\mathcal{H}$ 
12 Sample  $c_n \sim \text{Discrete}(\beta_{v_{nL}})$ 
13 Sample  $x_n \sim F(\theta_{c_n})$ 

```

Algorithm 1: GENERATIVE PROCESS OF BHMC (INFINITE)

$$\begin{aligned}
p(\mathbf{X} \mid \mathbf{V}, \Theta, \mathbf{B}) &= \prod_n \left(\sum_{k=1}^{\infty} \beta_{v_{nL}k} f(x_n; \theta_k) \right) \\
p(\mathbf{V} \mid \alpha) &= \Gamma(\alpha)^{|\mathcal{I}_{\mathcal{H}}|} \prod_{z \in \mathcal{I}_{\mathcal{H}}} \frac{\alpha^{m_z}}{\Gamma(N_z + \alpha)} \prod_{(z, z') \in E_{\mathcal{H}}} \Gamma(N_{z'}) \\
p(\mathbf{o} \mid \gamma_0) &= \prod_k \mathbb{B}(1, \gamma_0)^{-1} (1 - o_k)^{\gamma_0 - 1} \\
p(\mathbf{B}^- \mid \mathbf{V}, \gamma) &= \prod_{(z, z') \in E_{\mathcal{H}}} \mathbb{B}(\gamma \beta_z)^{-1} \prod_k \beta_{z'k}^{\gamma \beta_{zk} - 1} \\
p(\Theta \mid H) &= \prod_k p(\theta_k \mid H) \text{ (needs further specification)}
\end{aligned}$$

Fig. 2: The probabilities about the model

3 Regularised Solution

The PR framework was developed on top of variational inference (VI) for learning Bayesian models (Zhu et al., 2014b), i.e., as for VI, the goal is to minimise the KL-divergence (denoted by \mathbb{KL}) between a proposed distribution and the posterior distribution, but PR adds a penalty function based on a set of feature constraints to the optimisation problem.

Definition 1 (RegBayes) . Let $q(\mathbf{M})$ be a distribution proposed to approximate the posterior $p(\mathbf{M} | \mathbf{X})$. The PR method is to solve

$$\min_{q(\mathbf{M}), \boldsymbol{\xi}} \mathbb{KL}[q(\mathbf{M}) \parallel p(\mathbf{M}, \mathbf{X})] + U(\boldsymbol{\xi}, q, \mathbf{M}) \quad s.t. : q(\mathbf{M}) \in \mathcal{P}_{cs}(\boldsymbol{\xi})$$

where, $p(\mathbf{M}, \mathbf{X})$ denotes the joint probability of the model parameters and the data and $U(\boldsymbol{\xi}, q, \mathbf{M})$ is a penalty function obtained on the constraint space $\mathcal{P}_{cs}(\boldsymbol{\xi})$.

In the sequel, we will first discuss the specification of $\mathcal{P}_{cs}(\boldsymbol{\xi})$ and then $U(\boldsymbol{\xi}, q, \mathbf{M})$. Finally, we show the solutions.

3.1 PR specifications for BHMC

As discussed earlier, we aim to restrict the search space of the solution into a subspace that avoids some solutions where the separation between the siblings is too small. First, let us denote $\mathbf{M} = \mathbf{M}_0 \cup \{\boldsymbol{\eta}\}$ where $\{\boldsymbol{\eta}\}$ denotes a set of discriminant variables as discussed in Sec. 1.2. Now, let us extend Eq. (1) to a constraint space for HC. We can apply Eq. (1) for the assignment of the datum n at each level $1 \leq \ell \leq L$ rather than only at the leaf level. This imposes constraints in order to ensure that the hierarchy is well separated under each internal parent node. Recalling that $v_{n\ell}$ represents the correct node for datum n at level ℓ , the constraint space may be written as

$$\mathcal{P}_{cs}(\boldsymbol{\xi}) = \left\{ q(\mathbf{M}) \mid \begin{array}{l} 1 \leq n \leq N, 1 \leq \ell \leq L, \forall z \in \mathcal{S}(v_{n\ell}), \\ (\boldsymbol{\eta}_{v_{n\ell}} - \boldsymbol{\eta}_z)^\top \mathbf{x}_n \geq \epsilon_{n\ell}^\Delta - \xi_{n\ell}, \xi_{n\ell} \geq 0 \end{array} \right\} \quad (2)$$

where $\epsilon_{n\ell}^\Delta$ is the cost of choosing the child z over the true child $v_{n\ell}$.

To simplify the notation, let us denote an auxiliary variable:

$$\zeta_{n\ell z} := \epsilon_{n\ell} \mathbb{1}(z \neq v_{n\ell}) - (\boldsymbol{\eta}_{v_{n\ell}} - \boldsymbol{\eta}_z)^\top \mathbf{x}_n$$

where $\epsilon_{n\ell}^\Delta = \epsilon_{n\ell} \mathbb{1}(z \neq v_{n\ell})$. Notice that this is not a new variable but used for simplifying the notation. Based on the constrained space of Eq. (2), we design $U(\boldsymbol{\xi}, q, \mathbf{M})$ as the regularisation function:

$$U(\boldsymbol{\xi}, q, \mathbf{M}) = 2C \sum_n \max \left(0, \max_{\ell, z \in \mathcal{S}(v_{n\ell})} \mathbb{E}_q [\zeta_{n\ell z}] \right) \quad (3)$$

where C is a positive scale coefficient of the regularisation term and this is known as the hinge loss (Hastie et al., 2009). Heuristically, this regularisation function, plugged into a minimisation task, means to maximise ‘‘tightest separation’’ for an item from other paths by minimising the maximal margin violation between

the correct node at any level in the assigned path from its siblings. With this understanding, it suffices to set $\epsilon_{n\ell}$ as a constant hyperparameter ϵ_0 .

As the maximum function is convex, we instead consider minimising

$$\min_{q(\mathbf{M})} \mathbb{KL}[q(\mathbf{M}) \parallel p(\mathbf{M}, \mathbf{X})] + 2C \sum_n \mathbb{E}_{q(\mathbf{V}, \boldsymbol{\eta})} \left[\max \left(0, \max_{\ell, z \in \mathcal{S}(v_{n\ell})} \zeta_{n\ell z} \right) \right] \quad (4)$$

since $\max(0, \max_{\ell, z \in \mathcal{S}(v_{n\ell})} \mathbb{E}_q[\zeta_{n\ell z}]) \leq \mathbb{E}_q[\max(0, \max_{\ell, z \in \mathcal{S}(v_{n\ell})} \zeta_{n\ell z})]$. Again, \mathbf{V} is the set of path assignments to the observations. We can assume that the prior for all $\boldsymbol{\eta}_z$ is $p(\boldsymbol{\eta}_z) \sim \mathcal{N}(\mathbf{0}, \nu_0^2 \mathbf{I})$ given ν_0 as a hyperparameter.

Applying the variational derivations over the objective, one can obtain an analytical solution to $q(\mathbf{M})$.

Lemma 1 *The optimal solution of the objective in Eq. (4) is*

$$q(\mathbf{M}) \propto p(\mathbf{M} \mid \mathbf{X}) \prod_n \exp \left\{ -2C \max \left(0, \max_{\ell, z \in \mathcal{S}(v_{n\ell})} \zeta_{n\ell z} \right) \right\} \quad (5)$$

Lemma 1 has been proved through connecting the objective to the Euler-Lagrange equation and hence deriving the updates by setting its derivatives to 0 (Chen et al., 2014).

Discussion of alternative solution Another straightforward formulation of $U(\boldsymbol{\xi}, q, \mathbf{M})$ could be $\sum_n \sum_{\ell} \max_{z \in \mathcal{S}(v_{n\ell})} \mathbb{E}_q[\zeta_{n\ell z}]$, which indicates that we hope to separate the nodes under the parent at each level. However, one can change minimising this alternative penalty function to minimising its upper bound which is $L \max_{\ell} \max_{z \in \mathcal{S}(v_{n\ell})} \mathbb{E}_q[\zeta_{n\ell z}]$, since

$$\forall n : \sum_{\ell} \max_{z \in \mathcal{S}(v_{n\ell})} \mathbb{E}_q[\zeta_{n\ell z}] \leq L \max_{\ell} \max_{z \in \mathcal{S}(v_{n\ell})} \mathbb{E}_q[\zeta_{n\ell z}].$$

In practice, L can be simply absorbed into the coefficient C , and then we obtain the penalty function of Eq. (3). Additionally, from a hindsight regarding the inference, this setting has a clear advantage in the computational complexity for updating $\boldsymbol{\eta}$. For the adopted setting, each datum is associated with only one $\boldsymbol{\eta}_z$ in a path, while for the alternative version it would be used to compute updates for every $\boldsymbol{\eta}_z$ in the path.

4 Inference

We will employ the Markov Chain Monte Carlo method for inferring the model. In this section, we firstly specify the essential properties of the PR model and hence analyse the sampling details for the added variables. For most of the variables for the original model, sampling remains the same as in (Huang et al., 2021). We adopt the term RBHMC for the (posterior) regularised BHMC. The algorithmic procedure is displayed in Algorithm 2 and the missing derivations are exhibited in Sec. A of the Appendix.

4.1 Data augmentation

We denote by $s_n = (\ell, z)$, a tuple encapsulating the level ℓ and the sibling z that maximises $\zeta_{n\ell z}$. Then ζ_{ns_n} represents the maximum $\zeta_{n\ell z}$ corresponding to that tuple. Using the index, we let s_{n1} return the level and s_{n2} return the corresponding node. This is actually an idea inspired by the slice sampling (Chen et al., 2014). We write

$$p(s_n = (\ell, z) \mid \mathbf{v}_n, \boldsymbol{\eta}, \mathbf{x}_n) = \delta \left(\operatorname{argmax}_{\ell, z \in \mathcal{S}(v_{n\ell})} \zeta_{n\ell z} \right)$$

where $\delta(\cdot)$ is the Dirac delta function. This shows that s_n is determined, once \mathbf{v}_n is fixed.

To sample the regularised term, we have to appeal to data augmentation (Polson and Scott, 2011; Chen et al., 2014).

Polson and Scott (2011) showed that, for any arbitrary real ζ ,

$$\begin{aligned} \exp\{-2C \max(0, \zeta)\} &= \int_0^\infty \frac{1}{\sqrt{2\pi\lambda}} \exp\left\{-\frac{(C\zeta + \lambda)^2}{2\lambda}\right\} d\lambda \\ &\propto \int_0^\infty p(\lambda \mid \zeta) d\lambda \end{aligned} \quad (6)$$

where $p(\lambda \mid \zeta) \sim \mathcal{GIG}(1/2, 1, C^2\zeta^2)$ is a Generalised Inverse Gaussian (GIG) distribution, defined as

$$\mathcal{GIG}(x; \rho, a, b) \propto x^{\rho-1} \exp\{- (ax + b/x) / 2\}. \quad (7)$$

Introducing a set of augmented variables λ_n , such that

$$\begin{aligned} p(\lambda_n \mid \mathbf{v}_n, s_n, \mathbf{x}_n, \boldsymbol{\eta}) &\propto \frac{1}{\sqrt{\lambda_n}} \exp\left\{-\frac{(C\zeta_{ns_n} + \lambda_n)^2}{2\lambda_n}\right\} \\ &= \frac{1}{\sqrt{\lambda_n}} \exp\left\{-\frac{[C(\epsilon_0 \mathbb{1}(s_{n2} \neq v_{ns_{n1}}) - (\boldsymbol{\eta}_{v_{ns_{n1}}} - \boldsymbol{\eta}_{s_{n2}})^\top \mathbf{x}_n) + \lambda_n]^2}{2\lambda_n}\right\}, \end{aligned} \quad (8)$$

the objective of (4) is identical to the marginal distribution of the augmented post-data posterior:

$$q(\mathbf{M}_0, \boldsymbol{\eta}, \mathbf{s}, \boldsymbol{\lambda}) \propto \prod_n g(\mathbf{x}_n, \lambda_n \mid \mathbf{v}_n, s_n, \mathbf{B}, \boldsymbol{\Theta}, \boldsymbol{\eta}) p(\mathbf{M}_0, \boldsymbol{\eta}, \mathbf{s}) \quad (9)$$

where $\mathbf{s} = \{s_n\}_{n=1}^N$, likewise for $\boldsymbol{\lambda} = \{\lambda_n\}_{n=1}^N$. Additionally, the joint (pseudo) likelihood of \mathbf{x}_n and λ_n can be written as $g(\mathbf{x}_n, \lambda_n \mid \mathbf{v}_n, s_n, \mathbf{B}, \boldsymbol{\Theta}, \boldsymbol{\eta}) = p(\mathbf{x}_n \mid \mathbf{v}_n, \boldsymbol{\beta}_{v_{nL}}, \boldsymbol{\Theta}) p(\lambda_n \mid \mathbf{v}_n, s_n, \mathbf{x}_n, \boldsymbol{\eta})$. The target posterior $q(\mathbf{M}_0, \boldsymbol{\eta})$ can be approached by sampling from $q(\mathbf{M}_0, \boldsymbol{\eta}, \mathbf{s}, \boldsymbol{\lambda})$ and dropping the augmented variables.

4.2 Sampling (\mathbf{v}_n, s_n)

We appeal to the Metropolis-Hastings sampling for the path like that in (Huang et al., 2021). Meanwhile, we propose s_n along with \mathbf{v}_n . Let us denote $\varphi_n = (\mathbf{v}_n, s_n)$. For s_n , we obtain

$$s_n \mid \mathbf{x}_n, \mathbf{v}_n, \boldsymbol{\eta} = \operatorname{argmax}_{\ell, z \in \mathcal{S}(v_{n\ell})} \zeta_{n\ell z}.$$

The MH scheme considers an acceptance probability $\mathcal{A} = \min \left(1, \frac{\mathcal{P}' q(\varphi_n | \varphi'_n)}{\mathcal{P} q(\varphi'_n | \varphi_n)} \right)$ where \mathcal{P} denotes the posterior (including the regularisation) and the variable denoted with the prime superscript is that for the modified variable given the new proposal. We obtain

$$\frac{\mathcal{P}' q(\varphi_n | \varphi'_n)}{\mathcal{P} q(\varphi'_n | \varphi_n)} = \frac{g(\mathbf{x}_n, \lambda_n | \mathbf{v}'_n, s'_n, \mathbf{B}', \Theta, \boldsymbol{\eta})}{g(\mathbf{x}_n, \lambda_n | \mathbf{v}_n, s_n, \mathbf{B}, \Theta, \boldsymbol{\eta})}.$$

The derivation details are listed in Sec. A.1.

4.3 Sampling $\boldsymbol{\eta}_z$

Let us consider $(\lambda_n + C\zeta_{n\ell z})^2$ which is

$$\begin{aligned} (\lambda_n + C\zeta_{n\ell z})^2 &= \text{const.} - 2C(\lambda_n + C\epsilon_0)\boldsymbol{\eta}_{v_{n\ell}}^\top \mathbf{x}_n + 2C(\lambda_n + C\epsilon_0)\boldsymbol{\eta}_z^\top \mathbf{x}_n \\ &\quad + C^2\boldsymbol{\eta}_{v_{n\ell}}^\top \mathbf{x}_n \mathbf{x}_n^\top \boldsymbol{\eta}_{v_{n\ell}} - 2C^2\boldsymbol{\eta}_{v_{n\ell}}^\top \mathbf{x}_n \mathbf{x}_n^\top \boldsymbol{\eta}_z + C^2\boldsymbol{\eta}_z^\top \mathbf{x}_n \mathbf{x}_n^\top \boldsymbol{\eta}_z. \end{aligned}$$

We could hence sum up the terms over all datum, i.e. $\sum_n \mathbb{1}(v_{n\ell} = z \parallel s_{n2} = z) - \frac{(\lambda_n + C\zeta_{n\ell s_{n2}})^2}{2\lambda_n}$ for a certain $\boldsymbol{\eta}_z$.

On the other hand, the canonical parametrisation for a Multivariate Gaussian distribution can be written as

$$\mathcal{N}_{\text{canonical}}(\boldsymbol{\eta}_z | \boldsymbol{\nu}_z, \boldsymbol{\Lambda}_z) = \exp \left(\text{const.} + \boldsymbol{\nu}_z^\top \boldsymbol{\eta}_z - \frac{1}{2} \boldsymbol{\eta}_z^\top \boldsymbol{\Lambda}_z \boldsymbol{\eta}_z \right).$$

Therefore, let us combine the prior of $\boldsymbol{\eta}_z$ which is $\mathcal{N}(\mathbf{0}, \nu_0^2 \mathbf{I})$ together and then achieve

$$\begin{aligned} \boldsymbol{\nu}_z &= C^2 \left\{ \sum_{n:v_{n\ell}=z} \frac{1}{\lambda_n} \left(\left(\frac{\lambda_n}{C} + \epsilon_0 \right) \mathbf{x}_n^\top + \boldsymbol{\eta}_{s_{n2}} \mathbf{x}_n \mathbf{x}_n^\top \right) \right. \\ &\quad \left. - \sum_{n:s_{n2}=z} \frac{1}{\lambda_n} \left(\left(\frac{\lambda_n}{C} + \epsilon_0 \right) \mathbf{x}_n^\top - \boldsymbol{\eta}_{v_{n\ell}} \mathbf{x}_n \mathbf{x}_n^\top \right) \right\} \\ \boldsymbol{\Lambda}_z &= C^2 \sum_n \mathbb{1}(v_{n\ell} = z \parallel s_{n2} = z) \frac{\mathbf{x}_n \mathbf{x}_n^\top}{\lambda_n} + \nu_0^2 \mathbf{I}. \end{aligned}$$

The above term is in the natural exponent so that we can sample $\boldsymbol{\eta}_z$ by

$$\boldsymbol{\eta}_z | \mathbf{X}, \mathbf{s}, \boldsymbol{\lambda}, \mathbf{M} \setminus \{\boldsymbol{\eta}_z\} \sim \mathcal{N}(\boldsymbol{\Lambda}_z^{-1} \boldsymbol{\nu}_z, \boldsymbol{\Lambda}_z^{-1}).$$

4.4 Sampling λ_n

Based on Eq. (7), we sample $\lambda_n | \zeta_{n s_n}$ through $\mathcal{GIG}(1/2, 1, C^2 \zeta_{n s_n}^2)$ in our task. As shown in (Polson and Scott, 2011), if $x \sim \mathcal{GIG}(1/2, a, a/b^2)$ then $x^{-1} \sim \mathcal{IG}(|b|, a)$. Rather than sampling λ_n directly, this fact allows us to instead sample the reciprocal of λ_n from an Inverse Gaussian (IG) distribution: $\lambda_n^{-1} \sim \mathcal{IG}(|C\zeta_{n\ell s_{n2}}|^{-1}, 1)$.²

² This might mitigate the difficulty of seeking a mature library supporting GIG for some programming languages—but according to the authors' test, only R4.0.0 (compared with Python3.8 and Julia1.6) will not suffer from the numerical inconsistency when applying the reciprocal sampling from IG with very small C .

```

1 while not convergent do
2   foreach  $n \in \text{SHUFFLE}(N)$  do
3     Sample a path  $\mathbf{v}'_n$  and the corresponding  $\beta$  if needed
4      $s'_n \leftarrow \operatorname{argmax}_{1 \leq \ell \leq L, z \in \mathcal{S}(v_{n\ell})} \zeta_{n\ell z}$  //  $s'_n$  is the tuple of some  $\ell$  and  $z$ 
5     if  $\text{chance} \sim \text{Unif}(0, 1) < \mathcal{A}$  then //  $\varphi'_n = (\mathbf{v}'_n, s'_n)$ 
6       | Accept  $\varphi'_n$  and assign it to  $\varphi_n$ 
7     | Sample  $\lambda_n \mid \zeta_{ns_n}$ 
8   | Sample  $\mathbf{c}, \mathbf{B}, \Theta, \eta$ 

```

Algorithm 2: RBHMC SAMPLING PROCEDURE

4.5 Output hierarchy

In (Adams et al., 2010; Huang et al., 2021), the trees with the highest likelihood are output. In general for posterior estimation, one would like to present the output using the solution with the highest posterior during a finite number of MCMC draws. However, there are some works involving interesting discussions on replacing the highest posterior with other well-established criteria, e.g. (Rastelli and Friel, 2018; Wade and Ghahramani, 2018), etc. Their works focus on the flat clustering, and we leave this a future research challenge to explore a better criterion for choosing the output hierarchy under the Bayesian setting.

We follow Adams et al. (2010); Huang et al. (2021) and still apply the complete data likelihood (CDL) to select the output. This approach applies the regularised complete data likelihood (RCDL) where RCDL is defined as

$$p(\mathbf{X}, \mathbf{c}, \mathbf{V} \mid \mathbf{M} \setminus \{\mathbf{c}, \mathbf{V}\}) \prod_n \exp\{-2C \max(0, \zeta_{ns_n})\}.$$

Finally, any node with no siblings will be merged with its parent for presentation.

5 Experimental Study

We carry out an empirical study using the datasets evaluated in (Huang et al., 2021), on which hierarchies can be intuitively interpreted. We refer to these as the **Animals** and **MNIST-fashion** datasets. Principal Component Analysis (Hastie et al., 2009) is employed to reduce the dimension of the data to 7 and 10 respectively for the two datasets.

Sensitivity analysis

This analysis focuses on the regularisation parameters C and ϵ_0 for which hyperpriors are not appropriate (while the hyperparameter for η can have hyperpriors). From a statistical point of view, if C is too large then the regularisation term will dominate the pseudo likelihood. That is, the clustering should be close to a uniform assignment. When C approaches 0 (but note $C = 0$ in this solution will fail), the model can be regarded as the original BHMC.

The analysis aims to explore

- how sensitive the hyperparameters are;

- whether the algorithm can achieve improvements within some hyperparameter settings.

Thus, we examine two simple measures, 1) the expected average inner empirical L_2 distance within the nodes over multiple simulations, 2) the average centroid L_2 distance between the siblings. For simplicity, let us name the “inner” distance by AID, and the “outer” distance by AOD. For each set of hyperparameter configurations, we repeat 50 times and thus have AID as the expectation over $\text{AID}_{\text{single}}$, likewise for AOD. Specifically,

$$\text{AID}_{\text{single}} = \frac{1}{M} \sum_z \frac{2}{N_z(N_z - 1)} \sum_{\mathbf{x}_{n'}, \mathbf{x}_n \in z} \mathbb{1}(n > n') \|\mathbf{x}_n - \mathbf{x}_{n'}\|_2^2.$$

where M is the total number of non-root nodes in the hierarchy. Then, let $\mathbf{x}_{z_m}^{(c)}$ denote the centroid in a node m where $\mathbf{x}_{z_m}^{(c)} = \frac{1}{|z_m|} \sum_{\mathbf{x}_n \in z_m} \mathbf{x}_n$. Also let N_{sibs} be the set of sibling pairs under the same parent.

$$\text{AOD}_{\text{single}} = \frac{1}{N_{\text{sibs}}} \sum_{z: z \neq z_0} \sum_{z' \in \mathcal{S}(z)} \left\| \mathbf{x}_z^{(c)} - \mathbf{x}_{z'}^{(c)} \right\|_2^2.$$

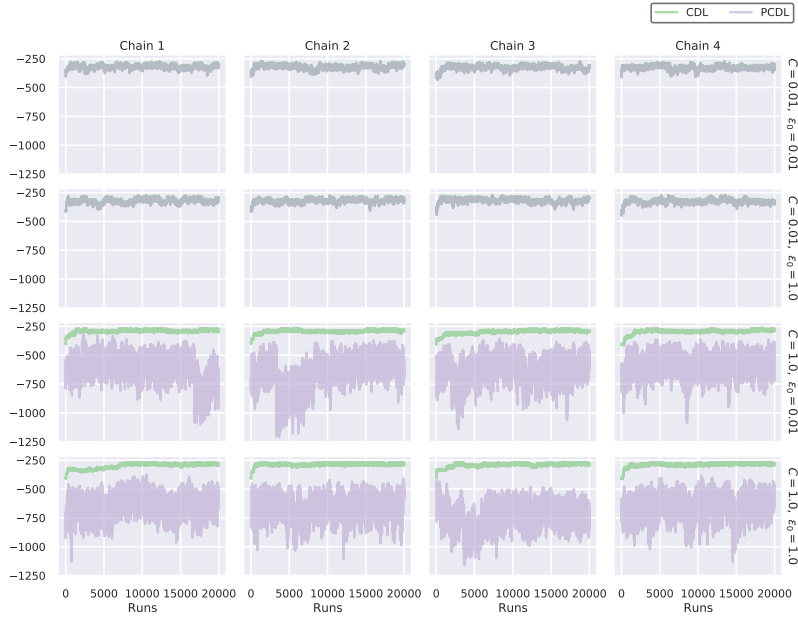
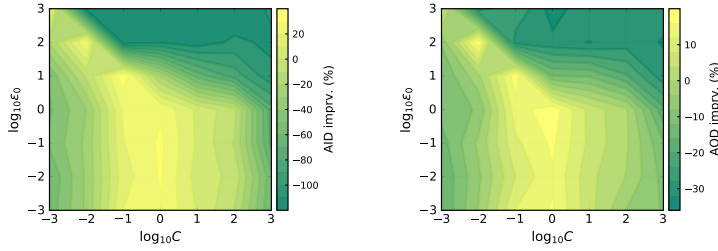
We would like to emphasise that, it is possible to have a random tree which has only one child under each parent (namely, a singular path), and in this case, AOD will fail. Therefore we exclude these cases which, fortunately, are rare. Finally, we consider the two measures together as any single measure could be affected by other factors, e.g. the number of nodes may enlarge the AID when there are fewer nodes. In summary, we would like to obtain a lower AID and a higher AOD.

5.1 Animals data

First of all, we fix the hyperparameters to $\alpha = 0.4, \gamma = 1, \gamma_0 = 0.85, L = 3, \nu_0 = 1, G = \mathcal{N}(\cdot, \mathbf{I}), H = \mathcal{N}(\mathbf{0}, \mathbf{I})$ which roughly follows the settings in (Huang et al., 2021).

Convergence analysis Fig. 3 shows the complete data likelihood (CDL) and the pseudo marginal complete data likelihood (PCDL). Each setting is run with 15,000 iterations. All of the plots show that both the statistics increase to a certain level while oscillating as more runs are carried out. Clearly, the variable C is the factor that influences the range of change for the PCDL. When $C = 0.01$, the PCDL and CDL are quite similar however, for $C = 1$, the fluctuations of the PCDL become far stronger. Some of the plots show that, even if the CDL seems smoothened, the PCDL still fluctuates strongly. This implies that the regularisation searches the space more effectively but the CDL is being kept at a rather consistent level.

Sensitivity analysis Fig. 4 depicts the sensitivity analysis for the two hyperparameters respectively. Again, each setting is run with 15,000 iterations. The tree in the last iteration is selected for computing the scores and thus is a random choice in some sense. It is unsurprising that the performance of either does not follow a linear relationship of the hyperparameters. We can find that there are certain settings for which the RBMHC achieves both a better AID and AOD, e.g. $C = 1$ and $\epsilon_0 = 1$.

Fig. 3: Convergence analysis on **Animals**Fig. 4: Sensitivity analysis on **Animals**

Meanwhile, it shows a number of choices that lead the RBHMC to outperform the original BHMC model. We can observe that the hyperparameter selections within a rather large numeric scale can provide an improved performance. It roughly follows the pattern that the smaller C and ϵ_0 lead to the stronger regularisation power.

Generally C is shown to be a more influential, yet setting a suitable ϵ_0 is still important.

Case analysis In this section, we run for a few hyperparameter settings with 5 chains. At each chain, we run the first 5,000 iterations as burnin, and report the hierarchy with the highest PCDL in the following 10,000 draws. For the BHMC, we report the one with the highest CDL.

As learned in Fig. 4, $(C = 1, \epsilon_0 = 1)$ and $(C = 0.01, \epsilon_0 = 1)$ are two good pairs of hyperparameter values. Therefore, we report two trees (from the first two MCMC chains) generated under these configurations and two trees from the the BHMC

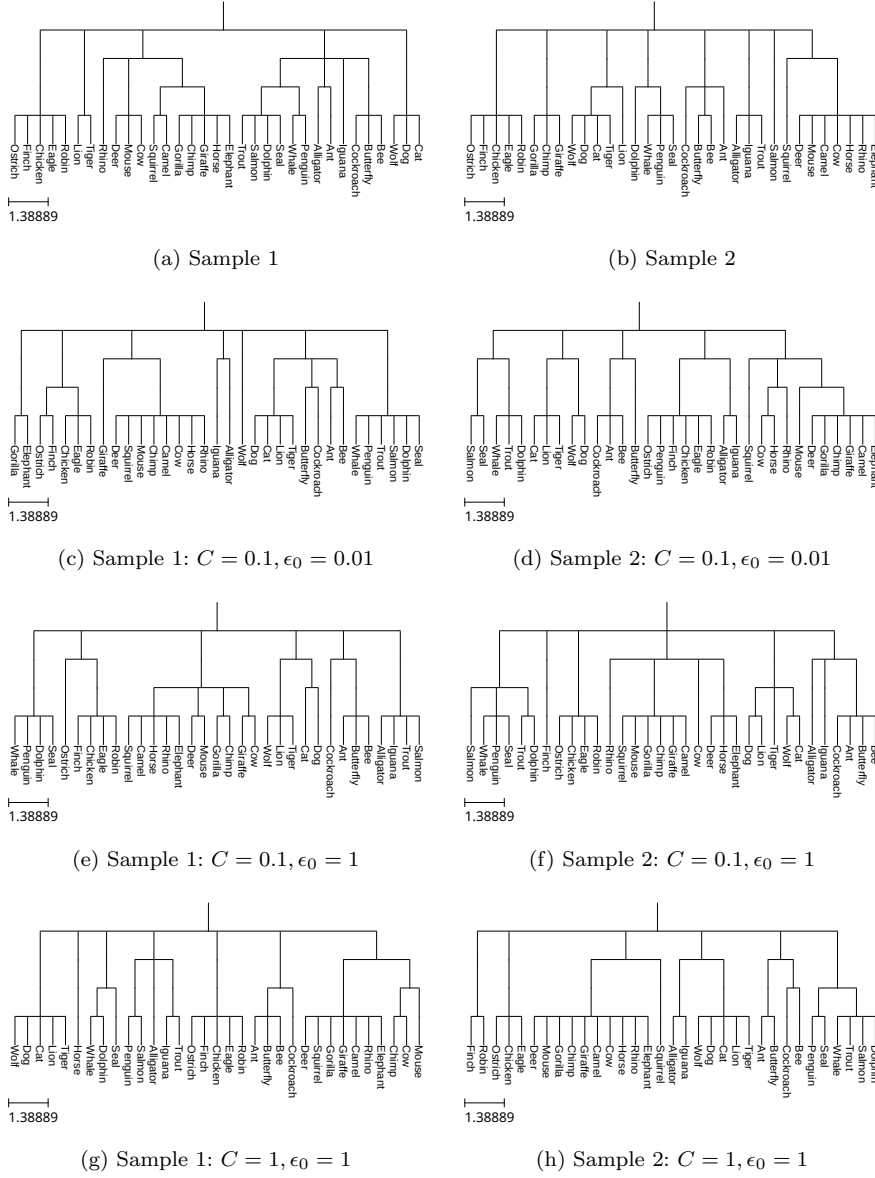
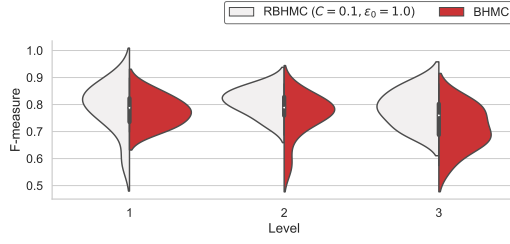
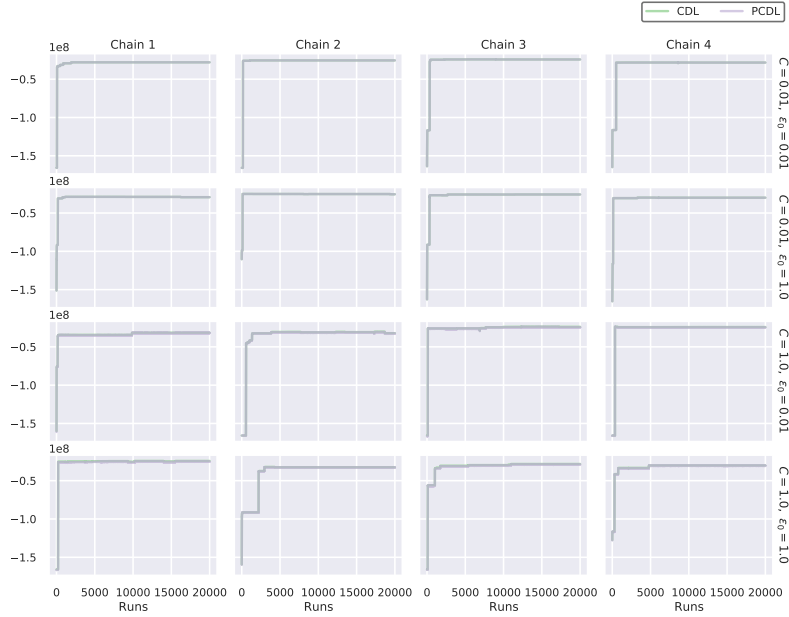


Fig. 5: Examples of output

model. We can see that BHMC has performed pretty well, while it still has some flaws for some cases, e.g. the sample 1 of the BHMC. For randomised clustering, it is understandable to have certain misplaced items. However, for RBHMC, they still look better under the randomised environment.

In (Huang et al., 2021), the experiments show that, even though BHMC performs very well in the lower levels, it might obtain a random combination of clusters in

Fig. 6: F-measure comparison for **Animals**Fig. 7: Convergence analysis on **MNIST-fashion**

higher levels which is due to the nature of the HDPMM. We would like to check if, with a good set of hyperparameters, RBHMC can achieve better performance than BHMC, particularly in higher levels, close to the root. We manually label the animals to the following classes: *birds*, *land mammals*, *predators*, *insects*, *amphibians*, *water animals*, *mouses*, and *fish* (further labelling is attached as a supplemental material). We then check the F-measure (Steinbach et al., 2000) against the clustering at each level. The RBHMC with ($C = 0.1, \epsilon_0 = 1.0$) and BHMC are run with 10 chains respectively, in which 5,000 burnin runs and 10,000 draws are carried out. Fig. 6 compares the F-measure by level for the two algorithms. The results at the first level show that, even though sometimes the RBHMC may perform worse than the BHMC, the distribution of scores for the RBHMC is skewed towards superior performance. For the later levels, it shows that the RBHMC performs even better though an original posit is that they should be on par.

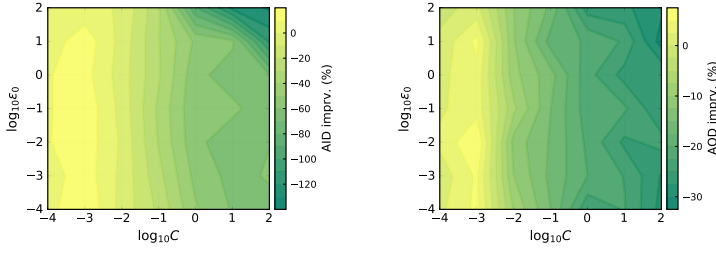


Fig. 8: Sensitivity analysis on MNIST-fashion

5.2 MNIST-fashion data

For this dataset, part of the hyperparameters are set as $\alpha = 0.2, \gamma = 1.5, \gamma_0 = 0.85, L = 4, \nu_0 = 1, G = \mathcal{N}(\cdot, \mathbf{I}), H = \mathcal{N}(\mathbf{0}, \mathbf{I})$.

Convergence analysis The CDL and RCDL of the algorithms for **MNIST-fashion** are demonstrated in Fig. 7. We run five chains with 5,000 burnin runs and 15,000 draws. In this example, we observe that the convergence of both CDL and RCDL is steadier. When $C = 1$, the variance of the RCDL is larger than that obtained when $C = 0.01$. However, all settings converge very nicely. Note that this data has 100 samples which might imply that with more data, the algorithm will have a stabler convergence performance.

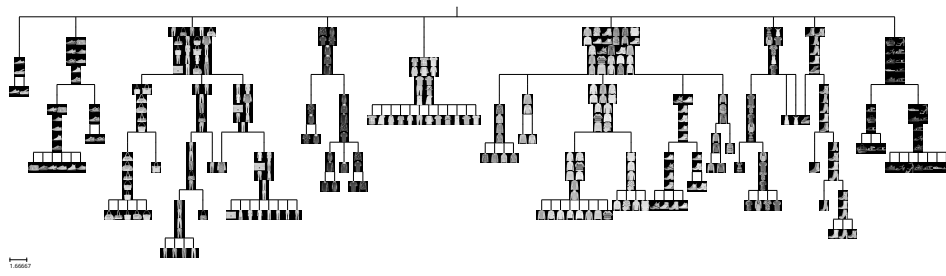
Sensitivity analysis We show the results in Fig. 8. Again, these experiments are run for 20,000 iterations. Each pair of C and ϵ_0 is repeated 50 times but the rare cases of having a singular path are eliminated. The scale of hyperparameters for achieving improvements are biased towards smaller values (in comparison with **Animals**). In agreement with the results for **Animals**, we can see that the improvement changes are smooth given the range of values. Moreover, it still illustrates that, within a certain range, we can obtain notable improvements as we expected. Still, the change of C affects the improvements more sensitively, though, we can not be careless about setting a suitable value for ϵ_0 .

Case analysis We run the hyperparameter settings for 4 chains and show the plots of the generated trees in Fig. 9.

We provide a poorly performed example generated from the setting $C = 1$ and $\epsilon_0 = 1$. Intuitively, with a larger C , it should be a uniform cluster allocations. In practice, this clustering is proposed by nCRP which follows the property that “the rich get richer” and thus we will more likely receive such a skewed hierarchy.

For BHMC, it returns a reasonable hierarchy but, e.g., the third cluster from the LHS is less well clustered. In regard to RBHMC, we deliberately show the results with $C = 0.001$ which is a value that results in improvements from Fig. 8. RBHMC results look better clustered.

The **MNIST-fashion** data has ground-truth labels in categories. We apply the same methodology as that for the **Animals** data. Again, 10 chains with 5,000 burn-in rounds and 10,000 draws are simulated. From the result in Fig. 10, we observe that at a higher level, the RBHMC has a potential to perform much better



(a) BHMC Sample

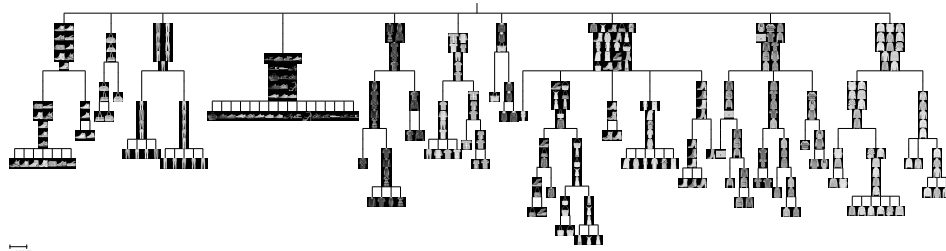
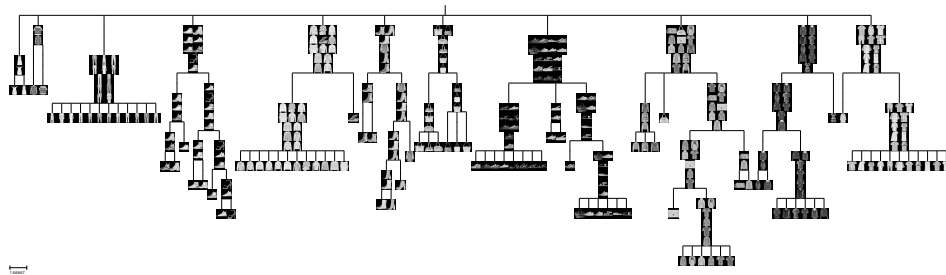
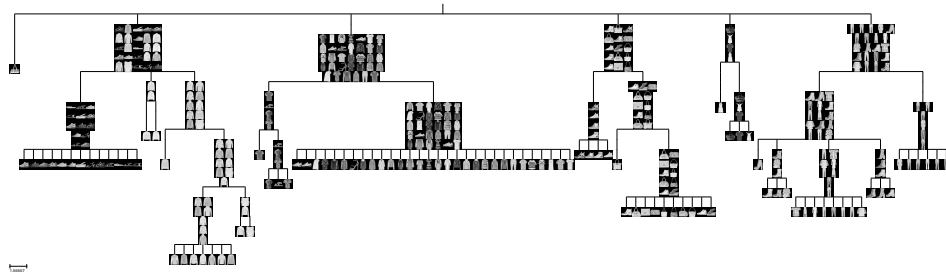
(b) Sample: $C = 0.001, \epsilon_0 = 0.01$ (c) Sample: $C = 0.001, \epsilon_0 = 1$ (d) Sample 1: $C = 1, \epsilon_0 = 1$

Fig. 9: Examples of output

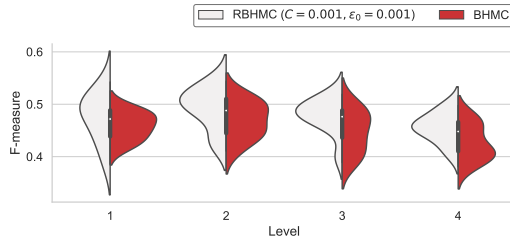


Fig. 10: F-measure comparison for MNIST-fashion

than the BHMC. The distributions of the RBHMC are also skewed towards better performance. For the lower level, the RBHMC outperform the BHMC even more.

6 Conclusion

In this work, we propose to apply posterior regularisation on the BHMC model to add *max-margin* constraints on the nodes of the hierarchy. We detail the modelling and inference procedures. The experimental study has shown its advantages over the original BHMC model and achieved the expected improvements. We expect this method could be employed to a broader range of Bayesian tasks. One future direction is to develop a variational inference approach over the regularised framework. It will also be interesting to investigate other penalty functions and features. Meanwhile, we should seek to extend the solutions to handle large scale problems.

Acknowledgements W. Huang, N. Laitonjam, and N. J. Hurley are supported by Science Foundation Ireland with the grant SFI/12/RC/2289_P2.

References

- Adams RP, Ghahramani Z, Jordan MI (2010) Tree-Structured Stick Breaking for Hierarchical Data. In: Advances in Neural Information Processing Systems 23, pp 19–27
- Altun Y, Smola A (2006) Unifying Divergence Minimization and Statistical Inference via Convex Duality. In: International Conference on Computational Learning Theory, Springer, pp 139–153
- Chen C, Zhu J, Zhang X (2014) Robust Bayesian Max-margin Clustering. In: Advances in Neural Information Processing Systems, pp 532–540
- Dudík M, Phillips SJ, Schapire RE (2004) Performance Guarantees for Regularized Maximum Entropy Density Estimation. In: Conference on Computational Learning Theory, vol 3120, pp 472–486
- Dudík M, Phillips SJ, Schapire RE (2007) Maximum Entropy Density Estimation with Generalized Regularization and an Application to Species Distribution Modeling. Journal of Machine Learning Research 8:1217–1260
- Ganchev K, Gillenwater J (2010) Posterior Regularization for Structured Latent Variable Models. Journal of Machine Learning Research 11:1998

- Graça JV, Ganchev K, Taskar B (2009) Expectation maximization and posterior constraints. *Advances in Neural Information Processing Systems 20 - Proceedings of the 2007 Conference* pp 1–8
- Hastie T, Tibshirani R, Friedman J (2009) *The Elements of Statistical Learning: Data Mining, Inference, and Prediction*. Springer Science & Business Media
- He J, Du C, Zhuang F, Yin X, He Q, Long G (2020) Online Bayesian max-margin subspace learning for multi-view classification and regression. *Machine Learning* 109(2):219–249
- Hsu CW, Lin CJ (2002) A Comparison of Methods for Multiclass Support Vector Machines. *IEEE transactions on Neural Networks* 13(2):415–425
- Huang W, Piao G, Moreno R, Hurley N (2020) Partially Observable Markov Decision Process Modelling for Assessing Hierarchies. In: *Asian Conference on Machine Learning (ACML)*, PMLR, pp 641–656
- Huang W, Laitonjam N, Piao G, Hurley N (2021) Inferring Hierarchical Mixture Structures: A Bayesian Nonparametric Approach. In: *Pacific-Asia Conference on Knowledge Discovery and Data Mining (PAKDD)*, Delhi, India
- Knowles DA, Ghahramani Z (2015) Pitman Yor Diffusion Trees for Bayesian Hierarchical Clustering. *IEEE Transactions on Pattern Analysis and Machine Intelligence* 37(2):271–289
- Neal RM (2003) Density Modeling and Clustering using Dirichlet Diffusion Trees. *Bayesian Statistics* 7:619–629
- Polson NG, Scott SL (2011) Data Augmentation for Support Vector Machines. *Bayesian Analysis* 6(1):1–23
- Rastelli R, Friel N (2018) Optimal Bayesian Estimators for Latent Variable Cluster Models. *Statistics and Computing* 28(6):1169–1186
- Steinbach M, Karypis G, Kumar V (2000) A Comparison of Document Clustering Techniques. In: *KDD Workshop on Text Mining*
- Sudderth EB (2006) *Graphical Models for Visual Object Recognition and Tracking*. PhD thesis, Massachusetts Institute of Technology
- Wade S, Ghahramani Z (2018) Bayesian Cluster Analysis: Point Estimation and Credible Balls (with Discussion). *Bayesian Analysis* 13(2):559–626
- Xie F, Xu Y (2020) Bayesian Repulsive Gaussian Mixture Model. *Journal of the American Statistical Association* 115(529):187–203
- Xu M, Zhu J, Zhang B (2012) Nonparametric Max-margin Matrix Factorization for Collaborative Prediction. *Advances in Neural Information Processing Systems* 25:64–72
- Zhu J, Xing EP (2009) Maximum Entropy Discrimination Markov Networks. *Journal of Machine Learning Research* 10(11)
- Zhu J, Chen N, Xing EP (2011) Infinite SVM: a Dirichlet Process Mixture of Large-margin Kernel Machines. In: *Proceedings of the 28th International Conference on Machine Learning (ICML-11)*, pp 617–624
- Zhu J, Ahmed A, Xing EP (2012) MedLDA: Maximum Margin Supervised Topic Models. *Journal of machine Learning research* 13(1):2237–2278
- Zhu J, Chen N, Perkins H, Zhang B (2014a) Gibbs Max-margin Topic Models with Data Augmentation. *Journal of Machine Learning Research* 15(1):1073–1110
- Zhu J, Chen N, Xing EP (2014b) Bayesian Inference with Posterior Regularization and Applications to Infinite Latent SVMs. *Journal of Machine Learning Research* 15:1799–1847

A Derivations

A.1 Acceptance probability

For computing the acceptance probability in the MH scheme, we obtain

$$\begin{aligned}
\frac{\mathcal{P}' q(\varphi_n | \varphi'_n)}{\mathcal{P} q(\varphi'_n | \varphi_n)} &= \frac{g(\mathbf{x}_n, \lambda_n | \mathbf{v}'_n, s'_n, \mathbf{B}', \Theta, \boldsymbol{\eta}) p(\mathbf{V}') p(\mathbf{B}')}{g(\mathbf{x}_n, \lambda_n | \mathbf{v}_n, s_n, \mathbf{B}, \Theta, \boldsymbol{\eta}) p(\mathbf{V}) p(\mathbf{B})} \frac{q(\mathbf{v}_n | \mathbf{v}'_n) q(\mathbf{B})}{q(\mathbf{v}'_n | \mathbf{v}_n) q(\mathbf{B}')} \\
&= \frac{g(\mathbf{x}_n, \lambda_n | \mathbf{v}'_n, s'_n, \mathbf{B}', \Theta, \boldsymbol{\eta}) p(\mathbf{v}'_n | \mathbf{V} \setminus \{\mathbf{v}_n\}) p(\mathbf{V} \setminus \{\mathbf{v}_n\})}{g(\mathbf{x}_n, \lambda_n | \mathbf{v}_n, s_n, \mathbf{B}, \Theta, \boldsymbol{\eta}) p(\mathbf{v}_n | \mathbf{V} \setminus \{\mathbf{v}_n\}) p(\mathbf{V} \setminus \{\mathbf{v}_n\})} \\
&\quad \times \frac{q(\mathbf{v}_n | \mathbf{v}'_n)}{q(\mathbf{v}'_n | \mathbf{v}_n)} \\
&= \frac{g(\mathbf{x}_n, \lambda_n | \mathbf{v}'_n, s'_n, \mathbf{B}', \Theta, \boldsymbol{\eta})}{g(\mathbf{x}_n, \lambda_n | \mathbf{v}_n, s_n, \mathbf{B}, \Theta, \boldsymbol{\eta})}
\end{aligned}$$

as $p(\mathbf{v}_n | \mathbf{V} \setminus \{\mathbf{v}'_n\}) = q(\mathbf{v}_n | \mathbf{v}'_n) = \text{nCRP}(\alpha)$, likewise for $p(\mathbf{v}'_n | \cdot)$ and $q(\mathbf{v}'_n | \mathbf{v}_n)$.

A.2 Sampling $\boldsymbol{\eta}_z$

First, we look at

$$\begin{aligned}
(\lambda_n + C\zeta_{n\ell z})^2 &= (\lambda_n + C\epsilon_0 - C(\boldsymbol{\eta}_{v_{n\ell}} - \boldsymbol{\eta}_z)^\top \mathbf{x}_n)^2 \\
&= (\lambda_n + C\epsilon_0)^2 - 2C(\lambda_n + C\epsilon_0)(\boldsymbol{\eta}_{v_{n\ell}} - \boldsymbol{\eta}_z)^\top \mathbf{x}_n \\
&\quad + C^2(\boldsymbol{\eta}_{v_{n\ell}}^\top \mathbf{x}_n - \boldsymbol{\eta}_z^\top \mathbf{x}_n)^2 \\
&= \text{const.} - 2C(\lambda_n + C\epsilon_0)\boldsymbol{\eta}_{v_{n\ell}}^\top \mathbf{x}_n + 2C(\lambda_n + C\epsilon_0)\boldsymbol{\eta}_z^\top \mathbf{x}_n \\
&\quad + C^2\boldsymbol{\eta}_{v_{n\ell}}^\top \mathbf{x}_n \mathbf{x}_n^\top \boldsymbol{\eta}_{v_{n\ell}} - 2C^2\boldsymbol{\eta}_{v_{n\ell}}^\top \mathbf{x}_n \mathbf{x}_n^\top \boldsymbol{\eta}_z + C^2\boldsymbol{\eta}_z^\top \mathbf{x}_n \mathbf{x}_n^\top \boldsymbol{\eta}_z.
\end{aligned}$$

We would like to point out that $\{n | v_{n\ell} = z\} \cap \{n | s_{n2} = z\} = \emptyset$ according to our constraint set. Hence, we need to sum up

$$\begin{aligned}
&\sum_{n: v_{n\ell}=z} \sum_{n: s_{n2}=z} -\frac{(\lambda_n + C\zeta_{n\ell s_{n2}})^2}{2\lambda_n} \\
&= C^2 \left\{ \sum_{n: v_{n\ell}=z} \frac{1}{\lambda_n} \left(\left(\frac{\lambda_n}{C} + \epsilon_0 \right) \mathbf{x}_n^\top + \boldsymbol{\eta}_{s_{n2}}^\top \mathbf{x}_n \mathbf{x}_n^\top \right) \right. \\
&\quad \left. + \sum_{n: s_{n2}=z} \frac{1}{\lambda_n} \left(- \left(\frac{\lambda_n}{C} + \epsilon_0 \right) \mathbf{x}_n^\top + \boldsymbol{\eta}_{v_{n\ell}}^\top \mathbf{x}_n \mathbf{x}_n^\top \right) \right\} \boldsymbol{\eta}_z \\
&\quad - \frac{1}{2} \boldsymbol{\eta}_z^\top \left\{ C^2 \sum_n \mathbb{1}(v_{n\ell} = z \parallel s_{n2} = z) \frac{\mathbf{x}_n \mathbf{x}_n^\top}{\lambda_n} \right\} \boldsymbol{\eta}_z + \text{const.}
\end{aligned}$$

B Labels for Animals

Table 1: Manual labels for **Animals**

animal	class
Elephant	land mammals
Rhino	land mammals
Horse	land mammals
Cow	land mammals
Camel	land mammals
Giraffe	land mammals
Gorilla	land mammals
Chimp	land mammals
Mouse	mouse
Squirrel	mouse
Tiger	predators
Cat	predators
Dog	predators
Wolf	predators
Lion	predators
Seal	water animals
Dolphin	water animals
Robin	birds
Eagle	birds
Chicken	birds
Salmon	fish
Trout	fish
Bee	insects
Iguana	amphibians
Alligator	amphibians
Butterfly	insects
Ant	insects
Finch	birds
Penguin	water animals
Cockroach	insects
Whale	water animals
Ostrich	birds
Deer	land mammals